Biochem. J. (1989) 262, 55–61 (Printed in Great Britain)

Heterogeneity of smooth endoplasmic reticulum from rat liver studied by two-phase partitioning

Peter GIEROW* and Bengt JERGIL†
Department of Biochemistry, Chemical Centre, University of Lund, P.O. Box 124, S-221 00 Lund, Sweden

Smooth microsomal membranes, prepared from rat liver by sucrose-density-gradient centrifugation, were subfractionated by counter-current distribution in an aqueous two-phase system consisting of poly(ethylene glycol) and Dextran T500. A comparison of the distribution curves of marker enzymes, together with theoretically calculated curves, indicated the presence of at least five membrane subfractions, differing in the ratios of the marker enzymes. Glucose-6-phosphatase and arylesterase distributed in one manner, and NADPH–cytochrome *c* reductase and NADH–ferricyanide reductase in another. Evidence for further heterogeneities in the distribution of marker enzymes in smooth microsomes was obtained by analysing the membrane domain structure using a recently described method [Albertsson (1988) Q. Rev. Biophys. **21**, 61–98]. Phenobarbital treatment did not influence the behaviour of the marker enzymes.

INTRODUCTION

When liver is homogenized the endoplasmic reticulum vesiculates. This appears to happen through active 'pinching off' (Palade & Siekevitz, 1956), leaving the lumenal contents within the vesicles formed. As a consequence, any lateral heterogeneity of the endoplasmic reticulum should be preserved and be manifest as vesicles of different compositions. By using fractionation methods which separate mainly according to size and density, smooth and rough microsomes have been isolated and characterized (for a review, see DePierre & Dallner, 1975). Extensive investigations of subfractions of rough microsomes separated by similar methods have shown the rough endoplasmic reticulum to be laterally heterogeneous (Svensson *et al.*, 1972; Beaufay *et al.*, 1974; Eriksson *et al.*, 1977; Amar-Costesec *et al.*, 1984). There are also some reports indicating heterogeneity of the smooth endoplasmic reticulum (Glaumann & Dallner, 1970; Lewis & Tata, 1973*a*). Such heterogeneities have been ascribed to structural differences between membrane regions which are rich and poor in ribosomes (Amar-Costesec & Beaufay, 1981), or to differentiation of the membranes into functional regions (DePierre & Dallner, 1975).

Counter-current distribution in aqueous two-phase systems has been used to separate plasma membrane domains (Gierow *et al.*, 1986), and also for testing theoretical models of membrane organization (Gierow *et al.*, 1988). This method, which separates membranes according to surface properties such as charge and hydrophobicity, has in these cases turned out to be a powerful tool for studying membrane heterogeneity. In this work, we have examined the heterogeneity of smooth microsomes by counter-current distribution; smooth rather than rough microsomes were examined in order to avoid heterogeneities due to the presence of ribosomes. The method has previously been used to fractionate microsomal membranes (Ohlsson *et al.*, 1978).

MATERIALS AND METHODS

Materials

Stock solutions of 20% (w/w) Dextran T500 (Pharmacia) and 40% (w/w) poly(ethylene glycol) 3350 (Carbowax 3350; Union Carbide) were prepared as described by López-Pérez *et al.* (1981). All other reagents were of analytical grade.

Preparation of smooth endoplasmic reticulum

A male Sprague–Dawley rat (150–200 g) was starved overnight and killed the following morning by cervical dislocation. The liver was immediately transferred to 2.5 vol. of ice-cold buffer containing 0.35 M-sucrose, 10 mM-$MgCl_2$, 25 mM-KCl, 0.1 mM-dithioerythritol and 50 mM-Tris/HCl, pH 7.4, cut into small pieces with a pair of scissors, and homogenized by six up-and-down strokes in a Potter–Elvehjem homogenizer. Smooth endoplasmic reticulum was isolated essentially as described by Lewis & Tata (1973*a*). The post-mitochondrial supernatant obtained was sedimented at 105000 *g* for 1 h, and the pellet suspended in the above buffer by 20 strokes in a Dounce homogenizer (pestle B, tight-fitting). An aliquot (12 ml) of the suspension was carefully layered on top of 10 ml of 0.9 M-sucrose and 15 ml of 1.3 M-sucrose (buffered as above) in Spinco SW-27 tubes. After centrifugation for 6.5 h at 95000 *g* in a Beckman SW27 swing-out rotor, the membranes at the 0.9/1.3 M-sucrose interface were collected, diluted 3-fold with 15 mM-LiOH and 1 mM-Tris/H_2SO_4, pH 7.8, and centrifuged at 105000 *g* for 1 h. The pellet obtained was suspended in minute amounts of the dilution buffer and immediately fractionated by counter-current distribution.

Some experiments involved rats injected intraperitoneally with phenobarbital, as described elsewhere (Ohlsson & Jergil, 1977), but otherwise treated as above.

Thin-layer counter-current distribution

Smooth microsomes (30 mg of protein) were added to

* Present address: Department of Physiology and Biophysics, University of Southern California, 1333 San Pablo Street, Los Angeles, CA 90033, U.S.A.
† To whom all correspondence should be addressed.

a sample system with a total weight of 8 g containing 5.9% (w/w) Dextran T500 and 5.9% (w/w) poly-(ethylene glycol) 3350, 10 mM-LiOH and 1 mM-Tris/H_2SO_4, pH 7.8. The bottom phase (see below) was added to obtain equal volumes of the two phases before sonication of the system, using a Branson Sonifer cell-disruptor, model B 15, equipped with a microtip. The intensity output was set to 3 and the pulsed duty cycle to 50%. The system was sonicated for 5 × 15 s, at intervals of 1 min, in an ice-water bath.

A standard thin-layer counter-current distribution apparatus equipped with a partition block with 60 cavities, numbered 0–59 (Albertsson, 1965, 1970), was loaded with the sample system and top and bottom phases essentially as described previously (Gierow *et al.*, 1986). The bottom phase capacity of the partition block was 0.79 ml, but in order to keep both the bottom phase and the interface stationary, only 0.71 ml was added of each of the two phases to cavities 5–59. The remaining five cavities (0–4) all received 1.42 ml of thoroughly mixed sample system. After completion of the separation cycle (about 11 h), 1 ml of 10 mM-Tris/HCl, pH 7.4, was added to each cavity, and the whole block was shaken for 1 min before unloading. The fractions obtained had to be analysed directly due to limited stability, particularly of glucose-6-phosphatase. Most enzyme activities diminished considerably upon freezing and thawing.

Assays

Protein was determined by the micro-assay of Bradford (1976), except that the difference between A_{595} and A_{465} was used to increase the sensitivity. Bovine serum albumin was used as a standard. The RNA content was measured by a modification of the method of Fleck & Munro (1962). The sample was precipitated in 5% trichloroacetic acid for 1 h, centrifuged for 10 min at 15 000 *g*, and the resulting pellet washed with 0.3 ml of trichloroacetic acid and processed as described.

The following endoplasmic reticulum enzymes were subjected to analysis: glucose-6-phosphatase (EC 3.1.3.9; Gierow & Jergil, 1980), NADPH–cytochrome *c* reductase (EC 1.6.2.4; Hrycay & O'Brien, 1974), NADH–ferricyanide reductase (EC 1.6.2.2; Hrycay & O'Brien, 1974) and arylesterase (EC 3.1.1.2; Shephard & Hubscher, 1969).

Theoretical curves

The experimentally obtained distribution curves were compared with theoretical curves calculated by a computerized method. The mathematical background has been desribed in detail elsewhere (Craig, 1962; Morris & Morris, 1976). Briefly, it requires the determination of the partition ratio, *G*, of the compound to be analysed. This could be calculated by using the experimentally determined amount of the compound in two consecutive fractions, $A_{n,i}$ and $A_{n,i+1}$, since:

$$\frac{A_{n,i+1}}{A_{n,i}} = \frac{(n-i)G}{i+1} \quad (1)$$

where n is the number of transfers (here 55), and i the fraction number. The G-value thus obtained is then used for calculating the theoretical amount, $T_{n,i}$, for each fraction, using the equation:

$$T_{n,i} = \frac{n!}{i! \times (n-i)!} \times \frac{G^i}{(1+G)^n} \quad (2)$$

By this method, several theoretical curves can be obtained and added until their sum matches the experimental curve.

The heterogeneity of the smooth endoplasmic reticulum was also analysed by a recently described method (Albertsson, 1988; Gierow *et al.*, 1988) where, for each fraction, the specific activities of pairs of enzymes were plotted against each other. From the shape of the resulting plot it is possible to draw conclusions about the distribution of the enzymes in a membrane relative to each other. Thus, a straight line with a positive slope is obtained when enzymes co-distribute, whereas distribution in different domains yields a negative slope. The slope of the plot also depends on the relationship between the size of the domain and fragment size (for a more detailed discussion see Albertsson, 1988; Gierow *et al.*, 1988).

RESULTS

A suitable composition of the phase system was first determined in a series of tubes containing varying amounts of polymers and of different ionic composition, as described elsewhere (Gierow *et al.*, 1986).

Four separate preparations of smooth endoplasmic reticulum were subjected to counter-current distribution,

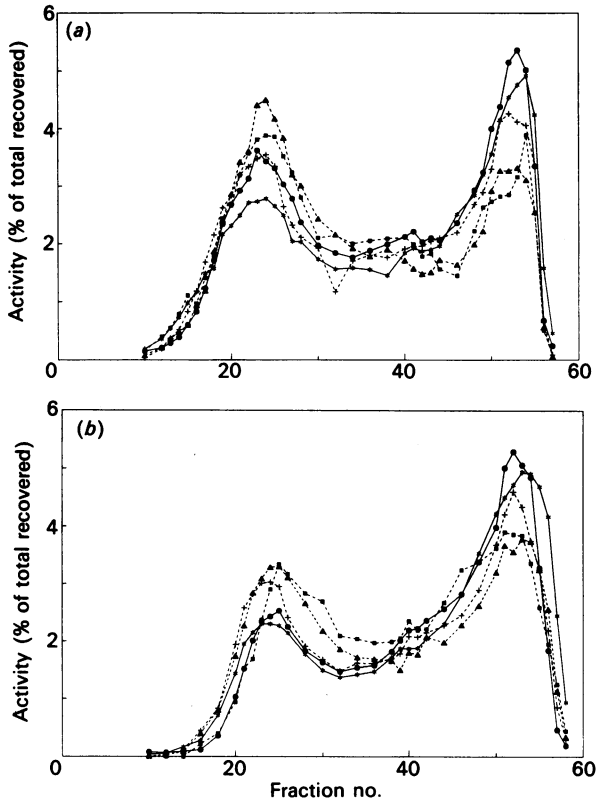

Fig. 1. Thin-layer counter-current distribution of smooth endoplasmic reticulum

The distribution was performed as described in the Materials and methods section. Marker enzyme activities and protein are expressed as percentages of the total amounts recovered. Distributions of arylesterase (▲), glucose-6-phosphatase (■), NADPH–cytochrome *c* reductase (+), NADH–ferricyanide reductase (●) and protein (*) are shown. (*a*) Untreated rats, (*b*) phenobarbital-treated rats.

Table 1. Specific activities of marker enzymes of smooth microsomes prepared from rat liver and recoveries after counter-current distribution

Specific activities for glucose-6-phosphatase and NADPH–cytochrome *c* reductase are expressed as nmol/min per mg of protein, and for NADH–ferricyanide reductase and arylesterase as μmol/min per mg of protein. Protein is expressed as mg/g of liver, RNA as mg/mg of protein, and recoveries as % of total added. The values are means ± S.D., or means ± deviation from the mean when $n = 2$. N.D., not determined; CCD, counter-current distribution.

Enzyme	Specific activity	Recovery after CCD (%)	*n*
Untreated:			
Glucose-6-phosphatase	176±22	60±24	4
NADPH–cytochrome *c* reductase	125±13	68±10	4
NADH–ferricyanide reductase	5.1±1.0	70±9	4
Arylesterase	6.1±1.1	85±12	4
Protein	3.4±0.6	116±14	4
RNA	0.10±0.02	N.D.	4
Phenobarbital-treated:			
Glucose-6-phosphatase	75±12	21±0.7	2
NADPH–cytochrome *c* reductase	233±22	70±8	2
NADH–ferricyanide reductase	5.9±0.1	67±0.4	2
Arylesterase	5.6±0.7	65±1	2
Protein	4.7±0.6	90±1	2
RNA	0.12	N.D.	1

Table 2. Partition ratio and frequency of components calculated from theoretical curves

Peak numbers refer to the numbers indicated in Fig. 2. *G* is the partition ratio and *P* the fraction of the enzyme in the different peaks (subpopulations), both expressed as means ± S.D. from four experiments.

Enzyme		Peak I	Peak II	Peak III	Peak IV	Peak V
Glucose-6-phosphatase	*G*	0.80±0.04	1.45±0.11	2.70±0.23	6.13±1.63	20.8±9.6
	P	0.39±0.03	0.18±0.03	0.14±0.01	0.15±0.04	0.16±0.05
NADPH–cytochrome *c* reductase	*G*	0.75±0.04	1.47±0.06	2.76±0.11	5.80±0.56	17.8±3.2
	P	0.35±0.05	0.15±0.02	0.16±0.02	0.16±0.02	0.18±0.04
NADH–ferricyanide reductase	*G*	0.78±0.05	1.47±0.07	2.63±0.09	5.88±0.57	17.0±3.2
	P	0.32±0.06	0.14±0.01	0.17±0.02	0.17±0.03	0.20±0.05
Arylesterase	*G*	0.78±0.02	1.53±0.10	2.71±0.21	5.90±0.82	19.0±4.3
	P	0.43±0.02	0.18±0.01	0.14±0.01	0.13±0.02	0.12±0.03

and the fractions obtained were analysed for marker enyme activities. A representative example of the highly reproducible distribution pattern is shown in Fig. 1(*a*). The pattern shows two major peaks containing different proportions of the four marker enzymes, and material with intermediate partition properties. More than 50% of the arylesterase activity was recovered in the left hand peak, whereas NADPH–cytochrome *c* reductase and NADH–ferricyanide reductase were located preferentially in the right hand peak, and glucose-6-phosphatase was more evenly distributed between the two peaks. More than 60% of the protein was recovered in the right hand peak. The recovery of enzyme activities after counter-current distribution was usually between 60 and 80%, glucose-6-phosphatase always being the lowest. Recovery of protein was above 90% (Table 1).

A closer examination of the distribution curves was performed by calculating theoretical distribution curves for the enzymes and comparing them with the experimentally obtained profiles (Figs. 2*a*–2*e*; Table 2). Both the enzymes and the protein could be resolved into at least five subpopulations. Arylesterase (Fig. 2*a*) and glucose-6-phosphatase (Fig. 2*b*) both showed a dominant peak to the left (peak I) representing 45–50% of the total activity. The rest of activity was rather evenly distributed between the remaining four peaks (II–V). The other two enzymes, NADPH–cytochrome *c* reductase (Fig. 2*c*) and NADH–ferricyanide reductase (Fig. 2*d*), showed a somewhat different pattern. The left hand peak (I) was relatively smaller, representing 30–35% of the total activity, with a corresponding increase in the right hand peaks (IV–V). This pattern was even more pronounced in the protein profile (Fig. 2*e*), where 40% was recovered in the two right hand peaks. In all curves, a better fit could be obtained by the introduction of a sixth peak to the left. This has not been done since such a peak most likely represents material 'tailing' in the apparatus as a thin film between the chamber or by adhesion to the walls.

Another, very sensitive, way of analysing hetero-

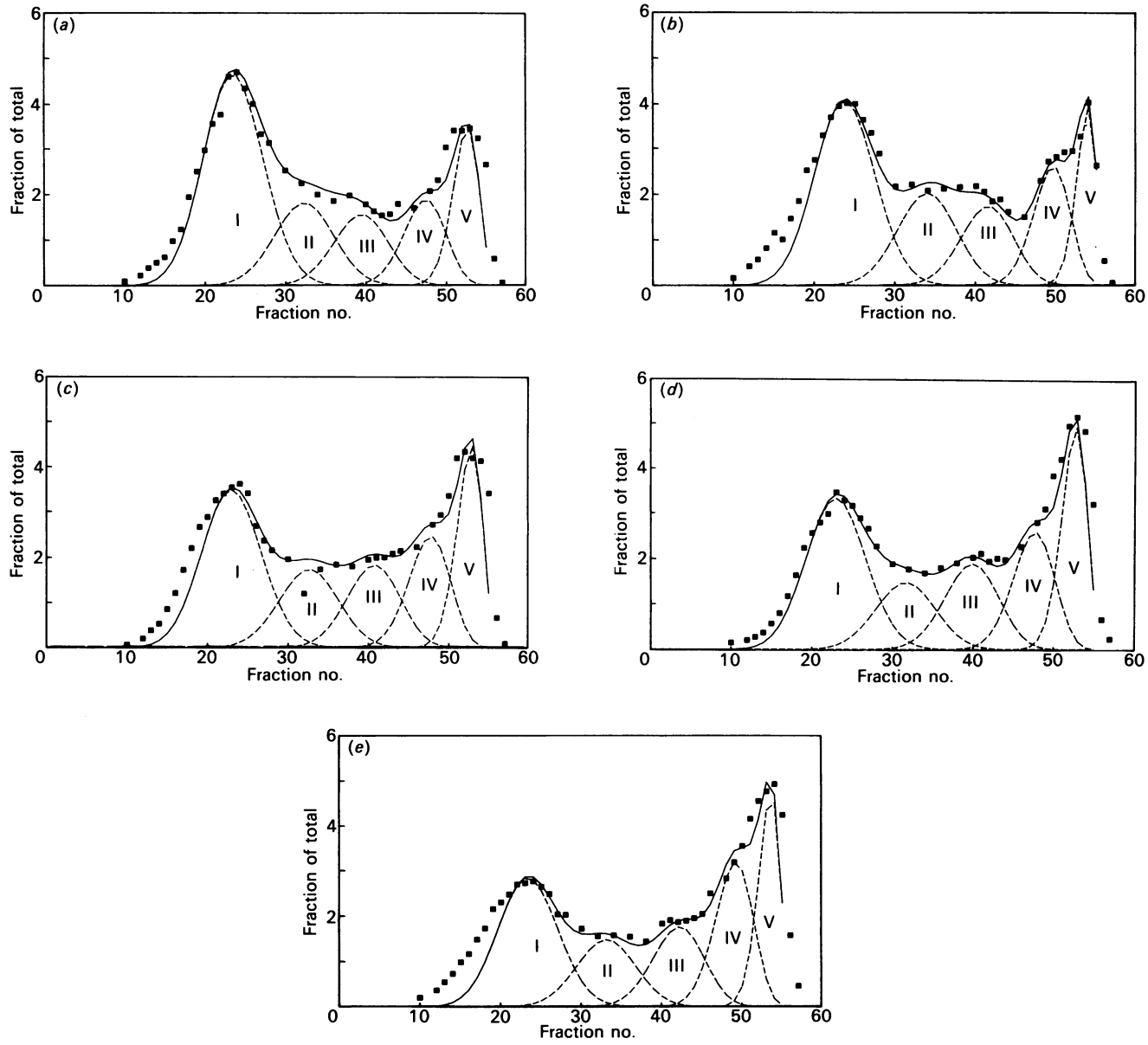

Fig. 2. Theoretical curves compared with experimental data

Each panel shows the experimentally obtained distribution of enzyme activity (■), the distribution of theoretically calculated populations (----, numbered I–V) and the sum of these populations (——). The distributions shown are (*a*) arylesterase, (*b*) glucose-6-phosphatase, (*c*) NADPH–cytochrome *c* reductase, (*d*) NADH–ferricyanide reductase and (*e*) protein.

geneities in the distribution of membrane components is to plot, for each fraction after counter-current distribution, the relative specific activity of one enzyme versus that of another (Albertsson, 1988; Gierow *et al.*, 1988). The heterogeneity of smooth endoplasmic reticulum was examined in this manner (Fig. 3) by replotting the results of Fig. 1. In most plots, no simple relationship was found between any of the enzyme pairs, bearing out the complexity of the membrane organization suggested by the theoretical plots.

When arylesterase was plotted against glucose-6-phosphatase (Fig. 3*a*), two straight lines of different positive slopes were obtained, one line (●) representing the left half and the other (○) the right half of the distribution curve. The lowest relative specific activities were observed in the far left and right ends of the distribution curve, and the highest in the middle fractions. This pattern of low and high specific activity was seen in all experiments conducted and was similar for all enzymes. The plot of NADPH–cytochrome *c* reductase versus NADH–ferricyanide reductase (Fig. 3*b*) also resulted in two straight lines of different positive slopes (fractions 12–19 and fractions 30–56 respectively), but these lines were connected by a third line representing fractions 19–30. The plots of arylesterase and glucose-6-phosphatase against NADH–ferricyanide reductase resulted in similar patterns (Figs. 3*c* and 3*d*), as did the plots of these enzymes against NADPH–cytochrome *c* reductase (Figs. 3*e* and 3*f*). In both cases the plots from the left as well as the right hand part of the distribution curve resulted in two lines at an angle.

The effect of phenobarbital treatment on the counter-

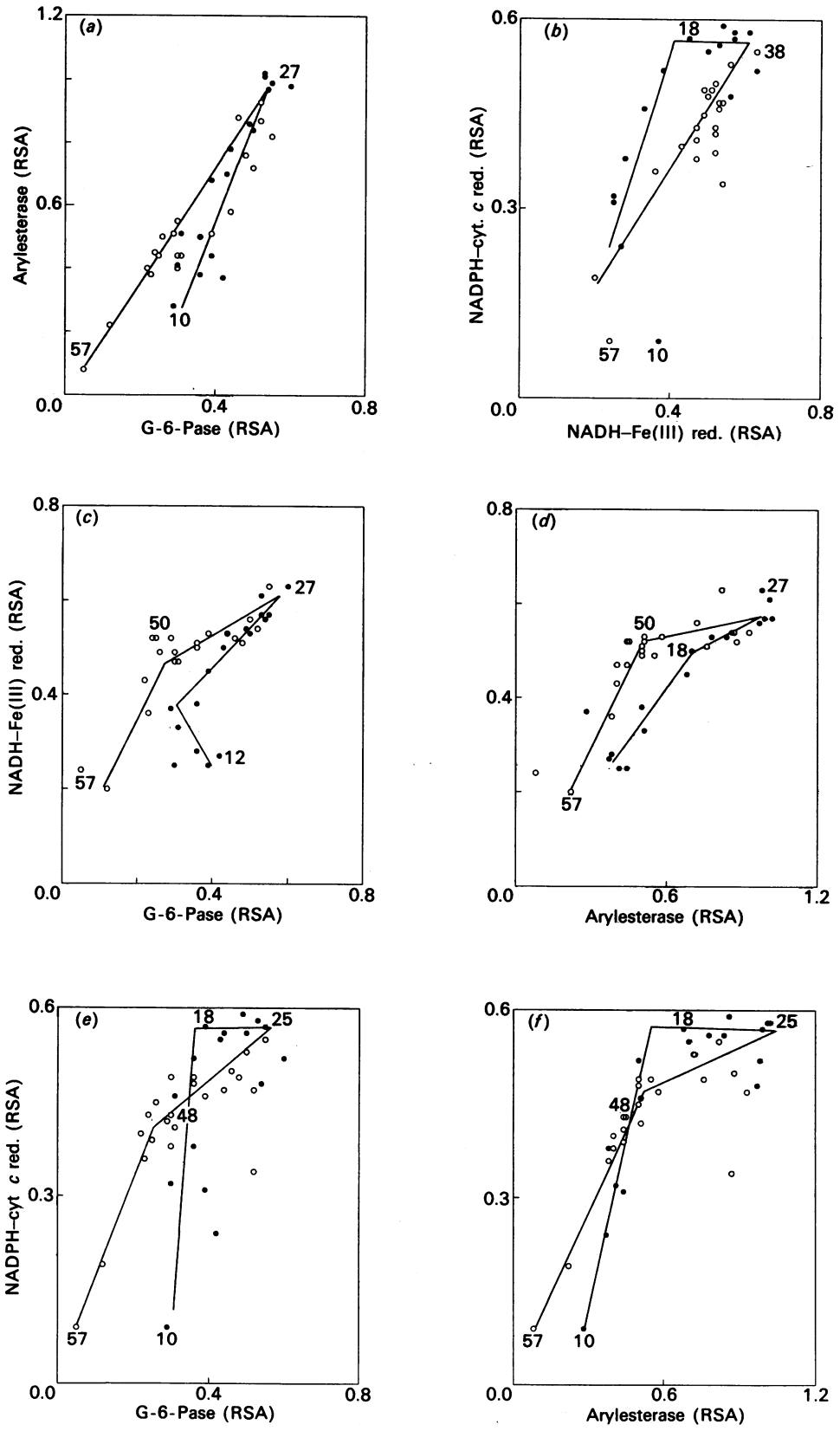

Fig. 3. Pairwise plots of relative specific enzyme activities

The relative specific activity (RSA) of an enzyme in each counter-current distribution fraction was calculated on the basis of the specific activity in the sample added, and plotted against the corresponding activity of another enzyme. ●, Fractions 10–27; ○, fractions 28–57 in Fig. 1. The numbers indicated represent fraction numbers. The lines are drawn arbitrarily, representing a general pattern obtained in all experiments. G-6-Pase, glucose-6-phosphatase, NADPH–cyt. *c* red., NADPH–cytochrome *c* reductase; NADH–Fe(III) red., NADH–ferricyanide reductase.

current distribution pattern of the marker enzymes in smooth microsomes was examined in two experiments. The treatment resulted in a 2-fold increase in the specific activity of NADPH–cytochrome *c* reductase, a decrease to less than half of glucose-6-phosphatase and no changes in the specific activities of NADH–ferricyanide reductase and arylesterase (Table 1). The counter-current distribution profiles of the enzymes from phenobarbital-treated rats did not differ perceptibly from those obtained from liver smooth microsomes of untreated rats (Fig. 1*b*). Furthermore, pairwise specific activity plots of the enzymes had the same shapes as those presented in Fig. 3 for untreated rats. This indicates that, although the treatment caused profound changes in the enzyme composition of the membrane, the distribution of the enzymes in the membrane relative to each other remained unchanged.

DISCUSSION

Smooth microsomes from rat liver could be fractionated by counter-current distribution into several populations having different proportions of marker enzymes. The analysis using theoretical curves indicated the presence of at least five membrane populations with different partition ratios. Less than five populations would result in deep troughs in the theoretical summation curves, which would then deviate from the experimental curves. The value is an approximation, however, due to some limitations in the theoretical treatment. First, a theoretical curve can be divided into several smaller ones, each one representing a different population. Second, the resolution is not constant throughout the distribution curve, i.e. relatively small differences in the partition ratio, *G*, are required to separate components recovered in the middle part of the curve (here fractions 20–40) compared with the far ends (fractions < 10 and > 50). Hence, peaks to the right might not have been resolved properly. Third, the program used for calculating the theoretical curves was designed for application of the sample in one cavity only, whereas we used five cavities to obtain measurable enzyme activities. Consequently, the 'true' theoretical curve should be the resulting profile of five curves, each one shifted stepwise to the right. But, as shown by Craig (1962), the resulting profile would only differ slightly, by being lower and somewhat broader, from the theoretical 'one-cavity' profile. Even considering these limitations, the theoretical analysis is a valuable tool in evaluating the complexity of the counter-current distribution curve.

Two different distribution patterns of the marker enzymes could be discerned by counter-current distribution. Glucose-6-phosphatase and arylesterase were more abundant relative to the two reductases in membranes distributing to the left (corresponding to peaks I and II in the theoretical curve of Fig. 2 and in Table 2), whereas the reductases were relatively more abundant to the right (peaks IV and V). Both the distribution curves and the specific activity plot of glucose-6-phosphatase against arylesterase (Fig. 3*a*) indicated that these enzymes co-distribute in smooth microsomes. The two reductases also followed each other rather closely in the distribution curve, but the more sensitive activity plot (Fig. 3*b*) indicated differences in their distribution. Similarly, the relative specific activity plots of glucose-6-phosphatase or arylesterase versus NADH–ferricyanide reductase or NADPH–cytochrome *c* reductase suggested heterogeneous distribution of these enzymes relative to each other.

A slightly different distribution in smooth microsomes between glucose-6-phosphatase on one hand and the two reductases on the other has been observed earlier by sucrose-density-gradient centrifugation (Glaumann & Dallner, 1970). Furthermore, there is cytochemical evidence that the glucose-6-phosphatase activity differs in various parts of smooth microsomes (Lewis & Tata, 1973*b*).

Several investigators have shown, by density-gradient centrifugation, that enzymes of rough endoplasmic reticulum distribute in two ways (Svensson *et al.*, 1972; Beaufay *et al.*, 1974; Eriksson *et al.*, 1977; Amar-Costesec *et al.*, 1984). Enzymes belonging to the electron transport system, which are exposed on the cytoplasmic surface, are more concentrated in membranes with low ribosomal content, whereas enzymes associated with the lumenal side, such as phosphatases and esterases, are more uniformly distributed throughout the membrane. It was suggested that the difference was due to physical exclusion of enzymes by ribosomes from certain membrane zones (Amar-Costesec & Beaufay, 1981). In contrast, enzymes associated with the lumenal side should be able to distribute more freely along the lateral plane of the membrane. Ribosome-dependent restrictions of the lateral movement of enzymes would not be expected in the smooth microsomal fraction with its low RNA content. Still, differences in the distribution of enzymes exposed on the lumenal and cytoplasmic sides of the membrane were observed in our experiments.

The picture emerging from the two-phase partitioning experiments is that the enzymes examined are widely distributed in the smooth endoplasmic reticulum. The counter-current distribution patterns, the theoretical curves and the plots of specific activities indicated that the four enzymes were present in all fractions, albeit in different proportions. As the microsomal membranes had been sonicated before counter-current distribution, the vesicle size was rather small (Svensson *et al.*, 1972). Thus, there was no evidence for large membrane zones devoid of any of these markers. As expected, this contrasts with the situation in plasma membranes, where regions with distinct enzyme composition could be discerned using the same analytical procedure (Gierow *et al.*, 1988). The induction experiments with phenobarbital, furthermore, showed that the organization of the enzymes in the smooth membrane was maintained, even though profound changes in their relative ratio were induced by the treatment. An explanation for the heterogeneity in the distribution of marker enzymes in smooth microsomes might be that enzymes distribute according to their function, as suggested by DePierre & Dallner (1975). To obtain information regarding this will require improved resolution and a larger selection of marker components.

We would like to thank Mrs. Hildegun Lundberg for technical assistance and Dr. Lars-Olof Persson for providing the computer program. This work was supported by a grant from the Swedish Natural Science Research Council.

REFERENCES

Albertsson, P.-Å. (1965) Anal. Biochem. **11**, 121–125
Albertsson, P.-Å. (1970) Sci. Tools **17**, 53–57

Albertsson, P.-Å. (1988) Q. Rev. Biophys. **21**, 61–98
Amar-Costesec, A. & Beaufay, H. (1981) J. Theor. Biol. **89**, 217–230
Amar-Costesec, A., Todd, J. A. & Kreibich, G. (1984) J. Cell Biol. **99**, 2247–2253
Beaufay, H., Amar-Costesec, A., Thinès-Sempoux, D., Wibo, M., Robbi, M. & Berthet, J. (1974) J. Cell Biol. **61**, 213–231
Bradford, M. M. (1976) Anal. Biochem. **72**, 248–254
Craig, L. C. (1962) in Comprehensive Biochemistry (Florkin, M. & Stotz, E. H., eds.), vol. 4, pp. 1–31, Elsevier, Amsterdam
DePierre, J. W. & Dallner, G. (1975) Biochim. Biophys. Acta **415**, 411–472
Eriksson, L. C., Bergstrand, A. & Dallner, G. (1977) Cell Tissue Res. **179**, 17–43
Fleck, A. & Munro, H. N. (1962) Biochim. Biophys. Acta. **55**, 571–583
Gierow, P. & Jergil, B. (1980) Anal. Biochem. **101**, 305–309
Gierow, P., Sommarin, M., Larsson, C. & Jergil, B. (1986) Biochem. J. **235**, 685–691
Gierow, P., Jergil, B. & Albertsson, P.-Å. (1988) Biochem. J. **249**, 369–375
Glaumann, H. & Dallner, G. (1970) J. Cell Biol. **47**, 34–48
Hrycay, E.-G. & O'Brien, P. J. (1974) Arch. Biophys. Biochem. **160**, 230–245
Lewis, J. A. & Tata, J. R. (1973*a*) J. Cell Sci. **13**, 447–459
Lewis, J. A. & Tata, J. R. (1973*b*) Biochem. J. **134**, 69–78
López-Pérez, M. J., Paris, G. & Larsson, C. (1981) Biochim. Biophys. Acta **635**, 359–368
Morris, C. J. O. R. & Morris, P. (1976) in Separation Methods in Biochemistry, 2nd edn., pp. 639–702, Pitman, London
Palade, G. E. & Siekevitz, P. (1956) J. Biophys. Biochem. Cytol. **2**, 671–690
Ohlsson, R. & Jergil, B. (1977) Eur. J. Biochem. **72**, 595–603
Ohlsson, R., Jergil, B. & Walter, H. (1978) Biochem. J. **172**, 189–192
Shephard, E. H. & Hubscher, G. (1969) Biochem. J. **113**, 429–440
Svensson, H., Dallner, G. & Ernster, L. (1972) Biochim. Biophys. Acta **274**, 447–461

Received 26 October 1988/20 March 1989, accepted 31 March 1989